

# Morphology and microstructure of Al–Li–Cu quasicrystals

A. R. KORTAN, H. S. CHEN, J. M. PARSEY Jr, L. C. KIMERLING  
AT&T Bell Laboratories, Murray Hill, New Jersey 07974, USA

Solidification microstructure of the stable icosahedral Al<sub>5.1</sub>Li<sub>3</sub>Cu alloy has been studied by scanning electron microscopy. Free surface solidification morphology was found to consist of heavily faceted dendrites with the shape of a triacontahedron. Quasicrystals grew fastest along the five-fold direction and the slowest growing two-fold planes gave rise to the faceted morphology. The differing growth conditions studied revealed the underlying growth mechanism. An epitaxial relationship between cubic and quasicrystalline phases was directly observed.

## 1. Introduction

One of the more remarkable discoveries [1] of recent times has certainly been that of the quasi-crystalline materials. However, important questions regarding the structure and formation of these materials still remain unanswered (for a recent review, see [2]). Independent of the preparation technique and the particular alloy system, this new class of materials exhibits a high density of defects which limits the long-range order to few tens of nanometres. Two significantly different models have been proposed to account for the observed icosahedral symmetry. The icosahedral glass model, first suggested by Schechtman and Blech [3] and later by Stephens and Goldman [4] is based on random packing of icosahedral clusters of atoms such that neighbouring clusters share vertices, edges or surfaces. The resulting structure strictly preserves the orientational order with a rather high density of defects. Tiling models [5], on the other hand, can generate a defect-free, perfect quasi-crystalline structure which would exhibit both orientational order and translational order. Refinements of each model, to give consistency with experimental results, have been introduced by increasing the correlations in a random glass model or increasing phason and dislocation-like defect densities in the tiling models.

The discovery [6] of the large-grain Al–Li–Cu icosahedral system has raised hopes of understanding the origins of the structural disorder. Despite the observed faceted morphology and macroscopic grain sizes [7], the long-range order in this system was again found [8] to be a few tens of nanometres. Here we report morphological studies of the Al–Li–Cu system which reveal the crystallographic nature of the disorder.

## 2. Results

### 2.1. Structure and thermodynamics

Shortly after the icosahedral symmetry of the Al–Li–Cu system was verified [8–10] by single-crystal X-ray diffraction, Pauling [11] suggested that the icosahedral structure could be explained by a multiply twinned

cubic structure. According to this model, the structure consists of twinned cubic crystals oriented around an icosahedral seed, such that 110 directions point along the radial directions and therefore the observed diffraction peaks in the Fibonacci series are of orders of  $hh0$ . Fig. 1 shows six diffraction peaks of a Fibonacci series of an equilibrium-grown Al–Li–Cu single quasicrystal, we measured by single-crystal X-ray diffraction technique. Two strong reflection positions 0/0 0/0 2/4 and 0/0 0/0 4/8 are matched to cubic indices (8 8 0) and (16 16 0) to define a cube of dimension 2.564 nm. Arrows in the figure indicate the predicted peak positions according to both quasicrystalline and Pauling's models. The measured peak positions are in very good agreement with the prediction of the quasi-crystalline theories [5, 12]. The twinning model, on the other hand, fails to provide an adequate description for peak positions other than 8 8 0 and 16 16 0 which were matched by us. We should note that the sample used in this measurement was grown under equilibrium

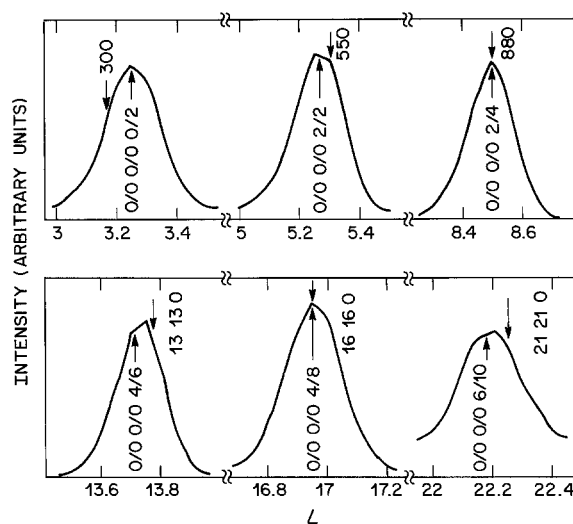


Figure 1 Single-crystal X-ray diffraction scans of icosahedral Al–Li–Cu system carried out along a two-fold zone axis showing six peak positions in a Fibonacci series. Arrows pointing up (down) indicate the positions of the 3DPT model (cubic twinning) predictions. Quasicrystalline models provide a better description.

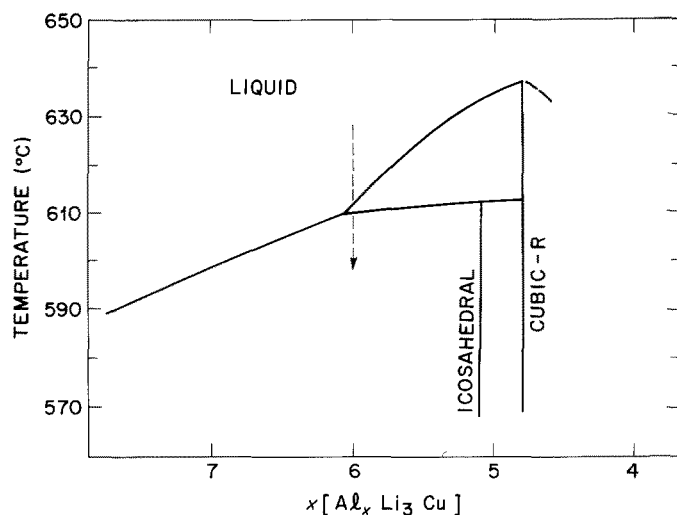


Figure 2 Partial phase diagram of Al-Li-Cu. The icosahedral phase is determined to be a non-congruently melting, thermodynamically stable phase. The composition of the sample used in morphological studies is indicated by the arrow.

conditions and showed no evidence for the peak position shifts that can be attributed to the presence of phason-like defects.

Recently, we have found [13] that the icosahedral phase (i-phase) of the Al-Li-Cu system is thermodynamically stable, and its formation follows a peritectic reaction with a composition of  $\text{Al}_{5.1}\text{Li}_3\text{Cu}$ . In the partial phase diagram shown in Fig. 2 the i-phase melts incongruently into the cubic-R and the liquid phases. An alloy melt with the right composition for the i-phase ( $\text{Al}_{5.1}\text{Li}_3\text{Cu}$ ) would therefore exhibit a strong cooling-rate dependence of the microstructure. If the cooling rate is too slow the cubic-R phase will nucleate, as the liquidus line of the R-phase is crossed, with a nucleation rate that will depend on the rate of cooling. The nucleated R-grains will then continually grow until the temperature reaches the freezing temperature of the i-phase, at which point the liquid will react with the R-phase to form the i-phase. Because this reaction is a very slow process, it is rarely completed before the remaining liquid solidifies. An R-phase grain that grows in this manner is therefore expected to be surrounded by a layer of i-phase.

It is possible to fast-cool through the liquidus region of the R-phase directly into the i-phase region of the phase diagram. In this case no R-phase grains will nucleate, and a highly undercooled liquid will solidify into the i-phase. Because the undercooling will usually be large, this procedure gives rise to a large nucleation rate and a small grain size for the i-phase.

This cooling-rate dependence of the different phase formations is often confused with the thermodynamic metastability of the icosahedral phases. Indeed, a metastable phase formation would have some similarity to the peritectic state, because both would be critically dependent on the cooling or the quench rates. A stable peritectic phase is distinguished, however, by the equilibrium growth conditions that exist on the solute-rich side of the phase diagram. If the melt composition is rich in solute (in our case  $x > 6.1$  for aluminium), such that by lowering the temperature we cross the liquidus line of the peritectic phase, the only phase that can nucleate will be the i-phase independent of the cooling rate. In this region one can choose an arbitrarily slow cooling rate to grow large grains. This method is precisely the technique that we have

employed [14] to grow single grains of inch-size dimensions ( $\sim 2.54$  cm).

## 2.2. Morphology

An alloy of  $\text{Al}_6\text{Li}_3\text{Cu}$  was prepared from research purity elements by induction melting in a helium atmosphere. The molten alloy in pyrolytical boron nitride crucible is then cast into another crucible, again in a helium atmosphere to induce directional solidification. After cooling the samples to room temperature, fractured pieces are mounted on an SEM Joel JSM-35C stage with silver paint for microstructural studies.

A large fraction of the sample surface is covered by 100 micrometre size faceted particles with an explicit two-fold axes truncated icosahedral symmetry. Fig. 3 shows such a well-isolated grain viewed along a five-fold rotational symmetry axis. The particle surface is composed of rhombi that are quite familiar from three-dimensional Penrose tiling (3DPT) models. The two basic tiles, prolate and oblate rhombohedrons, used in these constructions indeed are composed of the same rhombi that have an angle of  $63.43^\circ$  between the edges, which is the angle between two five-fold axes of an icosahedron. The geometric shape of the particle shown in Fig. 3 is known as a triacontahedron, a thirty-faced polyhedron which can be constructed from the two basic tiles used in 3DPT.

The faceted faces of the triacontahedron in Fig. 3 correspond to the two-fold quasi-crystallographic planes which appear to be not perfectly flat. There are two places on an individual facet where the flatness is disturbed: one, close to the five-fold corner, and another, in the middle of the rhombi, marked by E (eutectic) and D (dendritic) in Fig. 2. As we will demonstrate later, the features close to the five-fold vertices, D, are the tips of the last side branches of the main dendrites that terminate at the five-fold corners. The presence of these features suggests that these particles are indeed single-grain quasi-crystals and rules out the possibility [15] that the triacontahedron morphology may be a consequence of multiple twinning of some rhombohedral units. The feature observed at the middle of every face, E, is caused by the last solidifying piece of the liquid at the eutectic point. The details of this morphology become clear in Fig. 4

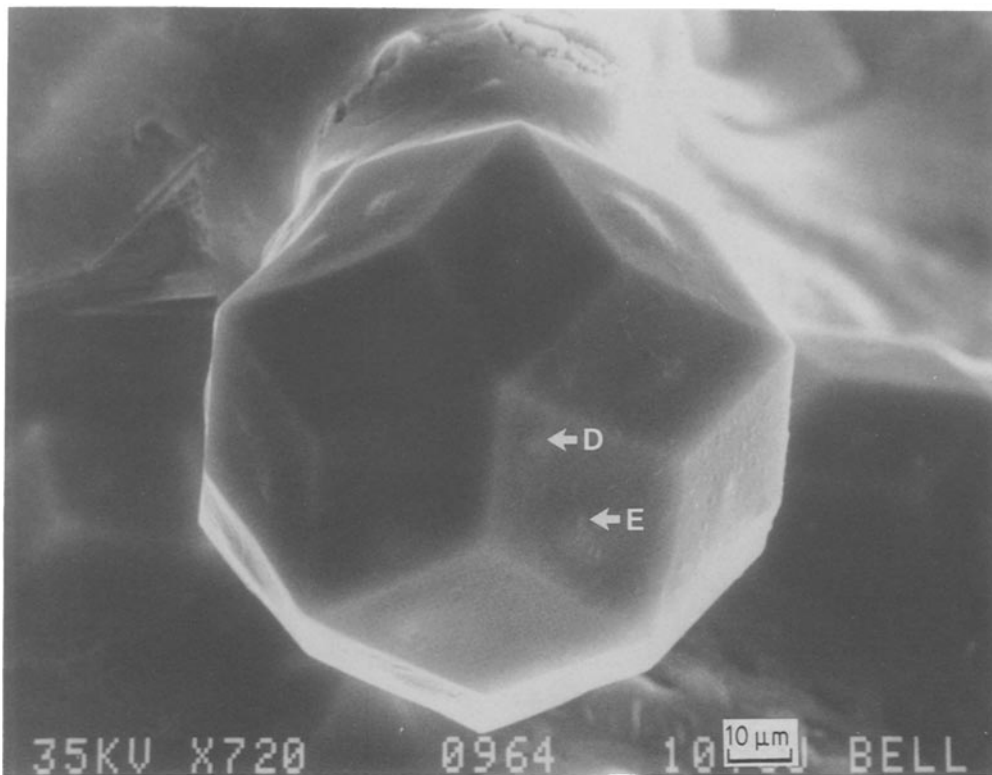


Figure 3 An isolated icosahedral phase single grain observed near the surface displaying its symmetry explicitly. The shape is that of a two-fold axes truncated icosahedron or a triacontahedron. Two types of features observed on two-fold facet planes, D and E, are explained in the text.

where another, more rapidly solidified particle is shown. Here every five-fold vertex point is clearly distinguishable with surrounding sharp facets, but the neighbouring facets are not entirely connected to define the two-fold planes. There are, in addition, voids at every three-fold symmetry point. These features can be understood by a dendritic growth mechanism that has highly anisotropic growth rates along the major symmetry directions. The five-fold

planes grow fastest, probably because they are the most loosely packed surfaces, while the two-fold planes grow slowest and limit the growth rate. Similar to ordinary crystals, the slowest growing planes define the morphology of the quasi-crystal and appear as facets. Once the icosahedral phase nucleates in the undercooled liquid, growth takes place along the six five-fold directions dendritically until the dendrites reach the surface. The solute rejected during growth

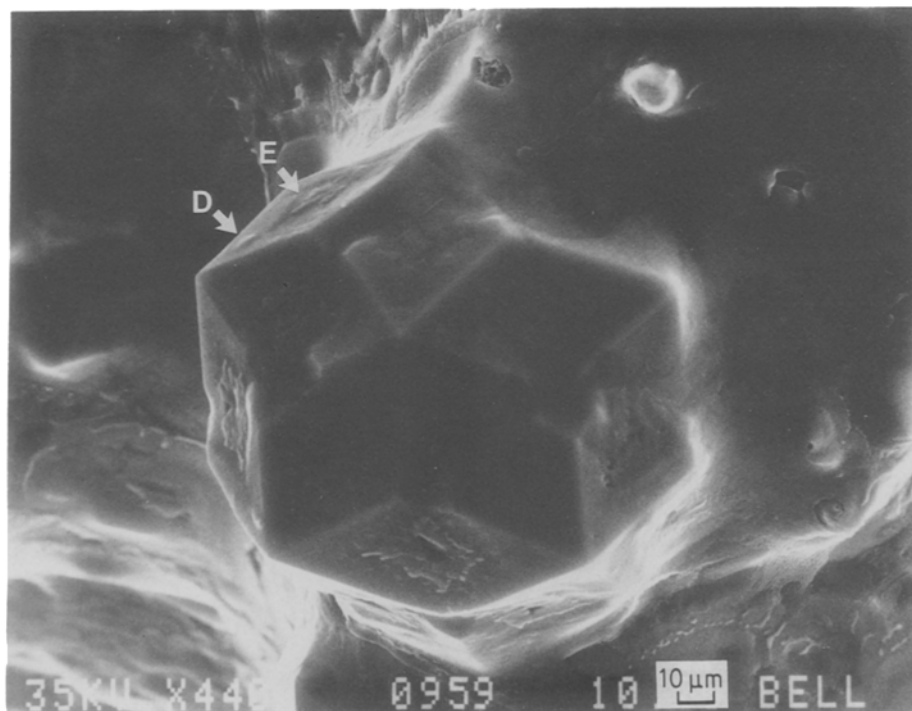


Figure 4 Another single icosahedral grain, grown more rapidly, reveals the details of the solidification morphology. The last solidifying liquid shown by E gets trapped between the six main dendrites that grow along the five-fold directions.

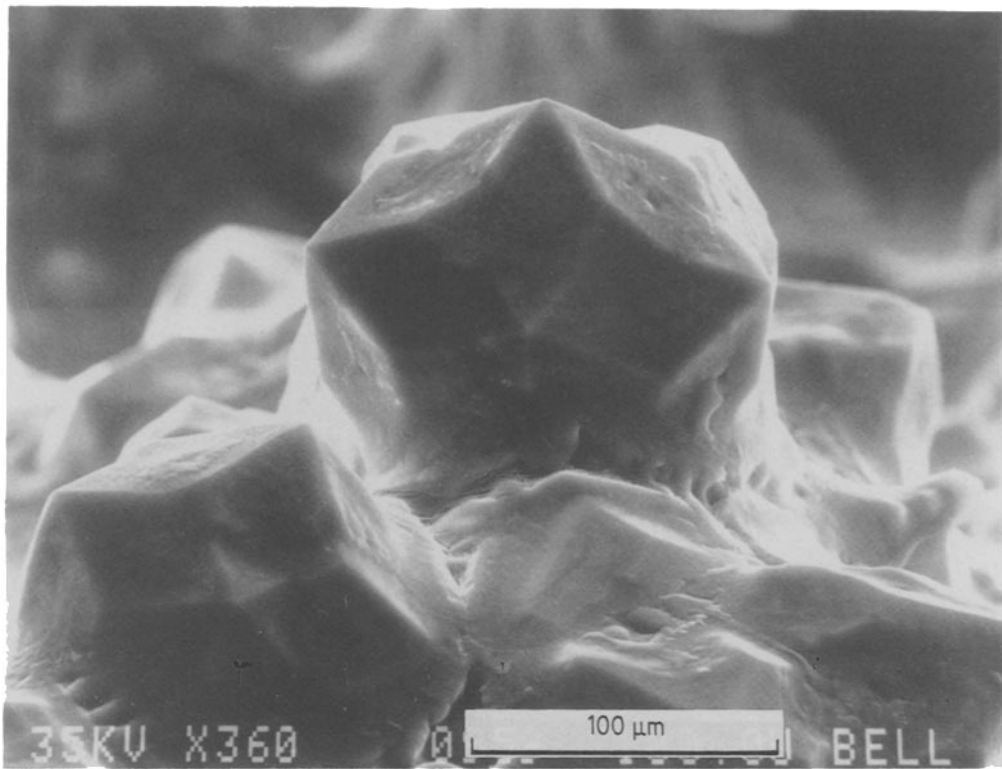


Figure 5 Several icosahedral grains all sharing a similar morphology indicate that growth primarily takes place along the six five-fold directions and is limited by the growth rate of the two-fold planes.

becomes the last solidifying liquid at the eutectic point and is trapped between the dendritic arms as shown by the features, E, on two-fold planes in Figs 4 and 5. Because all five-fold dendrite arms originate from the same seed they all share the same quasi-crystallographic orientations.

On relatively thin parts of the sample the morphology appears more dendritic as shown in Fig. 6. Presumably, the fast cooling of such regions produces

a very large undercooling of the melt, and the dendrites grow much faster. Dendrites that grow along the five-fold directions, therefore, appear more rounded except close to the tip where it remains faceted. Even at large undercoolings the growth rate is still governed by the growth rate of the two-fold planes.

In a shrink cavity we observed millimetre size dendrites grown along the five-fold directions as shown in Fig. 7. Here, the growth takes place completely in the

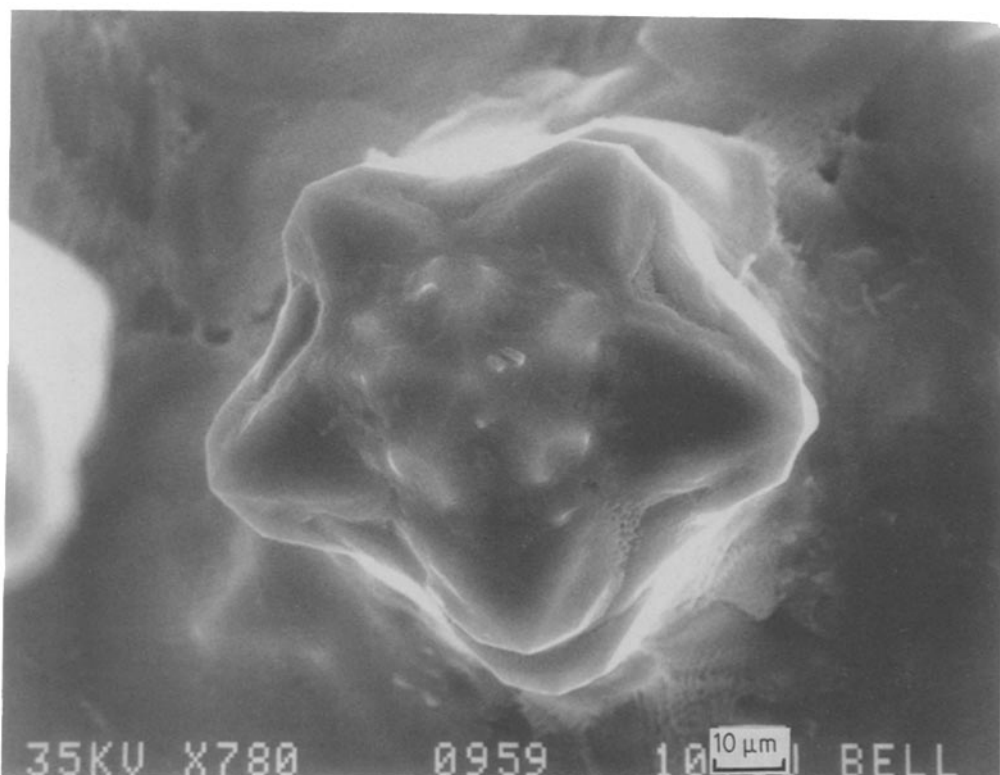


Figure 6 Morphology observed on thin parts of the sample appears even more dendritic where growth takes place faster. Here the five-fold primary dendritic trunks become well isolated. The faceting is only visible close to the dendrite tips.

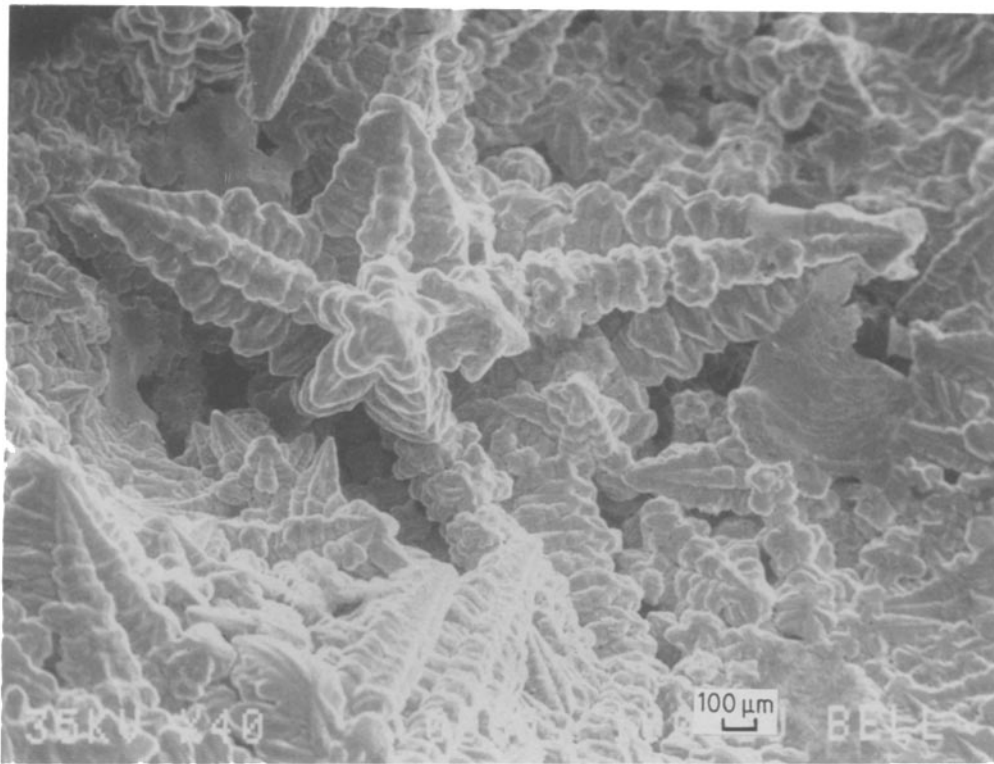


Figure 7 Dendritic microstructure of the icosahedral phase in a shrink cavity where the growth takes place in the melt. In melt grown samples icosahedral phase grows non-faceted.

melt. When growth is complete, the last freezing eutectic liquid shrinks in volume, exposing the peritectically-grown dendrites of the i-phase. Every dendrite and side branch observed are oriented along a five-fold direction, again indicating that this direction exhibits the fastest growth. Every side branch of dendrites that originate from the same seed share the same six five-fold directions which are defined by the main trunks. In the resulting pattern, side branches grow in the planes defined by two neighbouring main trunks.

The side branches closest to the tip are the ones that should show the facets near surface growth conditions as we mentioned earlier for Fig. 3. Most interestingly, facet formation by the two-fold planes is absent in these melt-grown crystals. Cross-sectional examinations of bulk quasicrystals grown from the melt at near-equilibrium conditions, also, display no faceting. Although the cubic-R phase always appears to grow highly faceted both in the melt and near the surface, the i-phase grains always grow dendritically in the

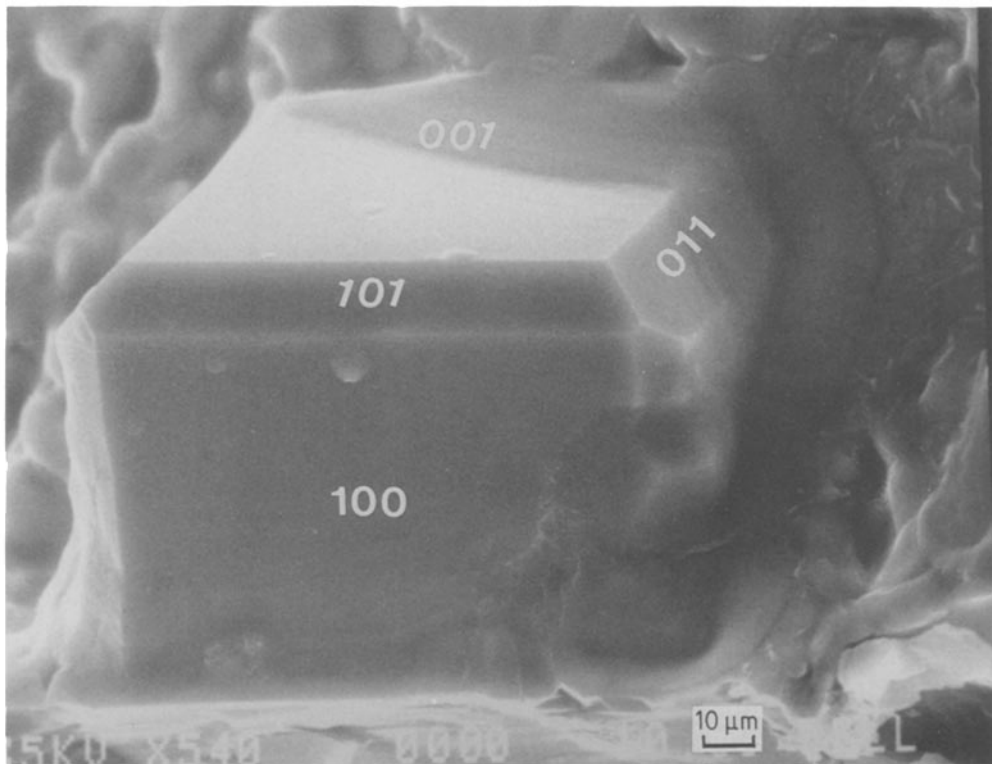


Figure 8 A single-crystal R-phase grain displaying (100) and (110) facet planes.

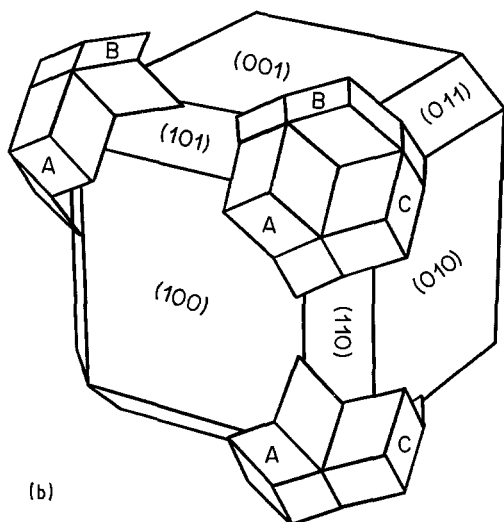
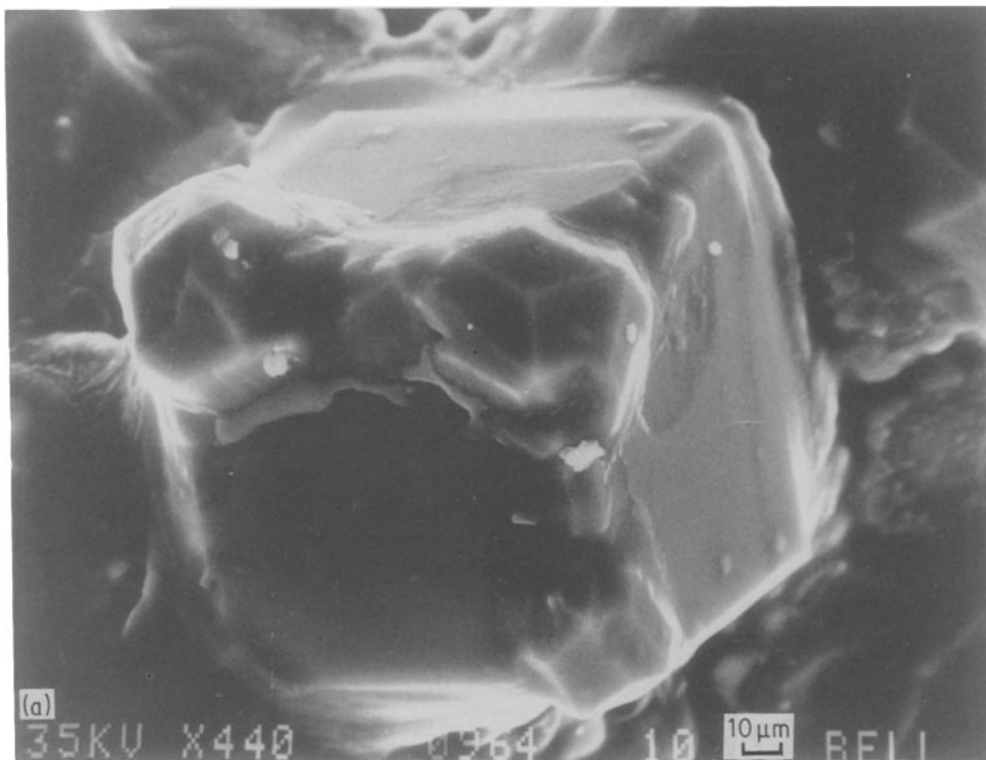


Figure 9 A single-crystal R-phase grain and three isolated but coherent icosahedral grains nucleated and grown on the (111) vertices (a). Three icosahedral grains are not only epitaxial with the cubic-phase but they all share the same orientation among themselves as shown in (b).

melt, even under equilibrium conditions. The rejected solute-rich region ahead of the growth interface produces a constitutional undercooling which undoubtedly plays a major role in creating instabilities at the interface and causes a dendritic growth. The large temperature gradient required to suppress the constitutional undercooling is very difficult to maintain in metallic systems; therefore we would expect to see the dendritic microstructure even for samples grown at near-equilibrium conditions. Noting that the cubic R-phase with a very similar entropy of fusion [13] to that of the i-phase ( $3.2$  and  $3.5 \text{ cal K mol}^{-1}$  for R and i phases, respectively) always grows faceted, both in the melt and near the surface, constitutional undercooling cannot account for the observed microstructural differences. The preferred dendritic growth of the i-phase is, therefore, possibly caused by a larger anisotropy in the growth-rate coefficients of the major symmetry planes. The facets only form surfaces where conditions are significantly different. We know from

metals that the nonfaceted melt growth morphology, with a typical entropy of fusion of 1, becomes heavily faceted under vapour growth conditions where the entropy of fusion increases by an order of magnitude. We, therefore, believe that the facet formation on surfaces is mostly caused by a vapour-phase growth mechanism.

The  $\text{Al}_6\text{Li}_3\text{Cu}$  alloy has a small temperature region near  $610^\circ\text{C}$  where it nucleates the cubic phase as shown in Fig. 2. In fact a small fraction of the grains we observed on the surface had a cubic morphology. These R-phase grains were about  $100 \mu\text{m}$  in size as shown in Fig. 8. The bounding surfaces were of (100) and (110) type indicating that (111) surfaces disappear by their fast growth and growth becomes limited by the growth rate of the (100) and (110) surfaces. Most fascinatingly, a few of these cubic grains had icosahedral quasicrystals epitaxially grown on them. Fig. 9a shows such a cubic grain with three quasicrystals coherently nucleated and grown from the (111) edges of the cube. There is a coherent epitaxy between the R- and i-phase grains such that the two-fold planes of the quasicrystals are aligned parallel to the (100) planes of the cubic grains while they share the same three-fold direction. This epitaxy fixes the five-fold axis of the i-phase parallel to the (530) cubic directions. To our knowledge this is the first direct observation of such an epitaxial relationship between the two phases.

Another very interesting observation is that the three separately nucleated grains all share the same

orientation. For a fixed three-fold direction one can align two-fold quasicrystalline planes with the (100) cubic planes in two distinct ways. As shown more explicitly in the representative model in Fig. 9b, the two-fold A planes of all i-phase grains that are parallel to (100) all share the same orientation. Similarly, B and C planes that are parallel to (001) and (010) cubic planes, respectively, also are aligned with respect to each other. This behaviour can be explained by taking a close look at the cubic phase structure, which belongs to the  $Mg_{32}(Zr, Al)_{49}$  (cI162) structure. This structure is made up of bcc packing of atomic clusters which have an internal icosahedral symmetry [16]. In this construction the two-fold symmetry axes of individual icosahedral clusters are collectively aligned along the (100) cubic planes. The four-fold rotational symmetry axes of the bcc structure, therefore, are two-fold symmetry axes when the internal symmetries of these clusters are considered.

### 3. Conclusion

The overall picture that emerges from this study is supportive of the tiling models. The facetting which is a natural consequence of the unit cell concept in condensed matter suggests the presence of similar building blocks for the icosahedral phase. The epitaxial relationship we observe between the i- and R-phases is a concept, uniquely of crystalline matter. The tiling model [12] demonstrates that, in fact, the same two basic tiles can be used to generate both crystalline and quasicrystalline structures.

### Acknowledgements

We thank K. A. Jackson and J. Dolan for helpful discussions.

### References

1. D. SHECTMAN, I. BLECH, D. GRATIAS and J. W. CAHN, *Phys. Rev. Lett.* **53** (1984) 1951.
2. D. GRATIAS (ed.), *J. Phys. Colloq.* **47-c3** (1986).
3. D. SHECHTMAN and I. BLECH, *Metall. Trans.* **16A** (1985) 1005.
4. P. W. STEPHENS and A. I. GOLDMAN, *Phys. Rev. Lett.* **56** (1986) 1168.
5. D. LEVINE and P. J. STEINHART, *ibid.* **53** (1984) 2477.
6. M. D. BALL and D. J. LLOYD, *Scripta Metall.* **19** (1985) 1065.
7. F. W. GAYLE, *J. Mater. Sci.* **22** (1987) 1.
8. A. R. KORTAN, H. S. CHEN and J. V. WASZCAK, *J. Mater. Res.* **2** (1987) 294.
9. C. BARTGES, M. H. TOSTEN, P. R. HOWELL and E. R. RYBA, *J. Mater. Sci.*, submitted.
10. P. A. BANCEL, P. H. HEINEY, P. M. HORN and F. W. GAYLE, in press.
11. L. PAULING, *Phys. Rev. Lett.* **58** (1987) 294.
12. C. L. HENLEY and V. ELSER, *Phil. Mag. B* **53** (1986) L59.
13. H. S. CHEN, A. R. KORTAN and J. M. PARSEY Jr, *Phys. Rev. B* **36** (1987) 7681.
14. J. M. PARSEY Jr, H. S. CHEN, A. R. KORTAN, F. A. THIEL, A. E. MILLER and R. C. FARROW, *J. Mater. Res.*, submitted.
15. P. GUYOT, *Nature* **326** (1987) 640.
16. G. BERGMAN, J. L. T. WAUGH and L. PAULING, *Acta Crystallogr.* **10** (1957) 254.

*Received 13 April  
and accepted 24 June 1988*